# Supersymmetric lepton flavor violation in low-scale seesaw models

**Ilakovac, Amon; Pilaftsis, Apostolos**

PHYSICAL REVIEW D **80,** 091902(R) (2009)

# Supersymmetric lepton flavor violation in low-scale seesaw models

Amon Ilakovac[1] and Apostolos Pilaftsis[2]

[1]*University of Zagreb, Department of Physics, Bijenička cesta 32, Post Office Box 331, Zagreb, Croatia*
[2]*School of Physics and Astronomy, University of Manchester, Manchester M13 9PL, United Kingdom*

(Received 22 April 2009; published 12 November 2009)

We study a new supersymmetric mechanism for lepton flavor violation in $\mu$ and $\tau$ decays and $\mu \to e$ conversion in nuclei, within a minimal extension of the minimal supersymmetric standard model with low-mass heavy singlet neutrinos and sneutrinos. We find that the decays $\mu \to e\gamma$, $\tau \to e\gamma$ and $\tau \to \mu\gamma$ are forbidden in the supersymmetric limit of the theory, whereas other processes, such as $\mu \to eee$, $\mu \to e$ conversion, $\tau \to eee$ and $\tau \to e\mu\mu$, are allowed and can be dramatically enhanced several orders of magnitude above the observable level by potentially large neutrino Yukawa coupling effects. The profound implications of supersymmetric lepton flavor violation for present and future experiments are discussed.

DOI: 10.1103/PhysRevD.80.091902 PACS numbers: 11.30.Hv, 12.60.Jv, 14.60.Pq

One of the best theoretically motivated scenarios of new physics is the minimal supersymmetric standard model, softly broken at the TeV scale. Its main virtues are that it provides a quantum-mechanically stable solution to the so-called gauge hierarchy problem, predicts gauge-coupling unification more accurately than the standard model does and offers a hopeful perspective for a consistent quantization of gravity by means of supergravity and superstrings [1].

Nevertheless, the low-energy sector of the minimal supersymmetric standard model needs be extended in order to accommodate the low-energy neutrino oscillation data. One popular extension is the one that realizes the famous seesaw mechanism [2], where the smallness of the observable neutrinos is counterbalanced by the presence of ultraheavy right-handed neutrinos $N_{1,2,3}$ with Majorana masses that are 2 to 4 orders of magnitude below the grand unification theory (GUT) scale $M_{\rm GUT} \sim 10^{16}$ GeV. The leptonic superpotential part for this extension is

$$W_{\rm lepton} = \hat{E}^C \mathbf{h}_e \hat{H}_d \hat{L} + \hat{N}^C \mathbf{h}_\nu \hat{L} \hat{H}_u + \hat{N}^C \mathbf{m}_M \hat{N}^C, \qquad (1)$$

where $\hat{H}_{u,d}$, $\hat{L}$, $\hat{E}$ and $\hat{N}^C$ denote the two Higgs-doublet superfields, the three left- and right-handed charged-lepton superfields and the three right-handed neutrino superfields, respectively. Note that the Yukawa couplings $\mathbf{h}_{e,\nu}$ and the Majorana mass parameters $\mathbf{m}_M$ are $3 \times 3$ complex matrices. In a minimal supergravity seesaw model, lepton flavor violation (LFV), such as $\mu \to e\gamma$ and $\mu \to eee$, originates from off-diagonal renormalization-group effects induced by the neutrino Yukawa couplings $\mathbf{h}_\nu$ on the soft supersymmetry (SUSY) breaking mass matrices $\tilde{\mathbf{M}}^2_{L,E}$ and the trilinear couplings $\mathbf{h}_e \mathbf{A}_e$ [3,4]. However, if the soft SUSY-breaking parameters $\tilde{\mathbf{M}}^2_{L,E}$ and $\mathbf{A}_e$ were flavor diagonal or proportional to the 3-by-3 identity matrix $\mathbf{1}$ at $\mathbf{m}_M \approx m_N \mathbf{1}$, with $m_N \gtrsim 10^{12}$ GeV, all low-energy charged LFV phenomena would be extremely suppressed by factors $m_\nu/m_N$ [5], where $m_\nu \lesssim 0.1$ eV is the light-neutrino mass scale.

In this article we study a new supersymmetric mechanism for lepton flavor violation (SLFV) which becomes dramatically enhanced in low-scale seesaw extensions of the minimal supersymmetric standard model. As we will show, the new important feature of SLFV is that it does not vanish in the supersymmetric limit of the theory, giving rise to distinctive predictions for charged LFV in present and future experiments, such as MEG [6] and PRISM [7].

In low-scale seesaw models of interest here [8–11], the smallness of the light-neutrino masses is accounted for by natural, quantum-mechanically stable cancellations due to the presence of approximate lepton flavor symmetries [11,12], while the Majorana mass scale $m_N$ can be as low as 100 GeV. Most interestingly, in these models LFV transitions from a charged lepton $l = e, \mu, \tau$ to another $l' \neq l$ are generically enhanced by the ratios [13–15]

$$\mathbf{\Omega}_{ll'} = \frac{v_u^2}{2m_N^2} (\mathbf{h}_\nu^\dagger \mathbf{h}_\nu)_{ll'} \qquad (2)$$

and are not constrained by the usual seesaw factor $m_\nu/m_N$, where $v_u/\sqrt{2} \equiv \langle H_u \rangle$ is the vacuum expectation value of the Higgs doublet $H_u$, with $\tan\beta \equiv \langle H_u \rangle / \langle H_d \rangle$. Here we will set limits on the off-diagonal entries of $\mathbf{\Omega}_{e\mu}$, $\mathbf{\Omega}_{\mu\tau}$ and $\mathbf{\Omega}_{e\tau}$ that are derived from the nonobservation of LFV in $\mu$ and $\tau$ decays and of $\mu \to e$ conversion in nuclei [16].

To be able to understand the profound implications of SLFV, we assume that the singlet neutrino sector of the low-scale seesaw model is exactly supersymmetric. This assumption is a good approximation, as long as $m_N \gg M_{\rm SUSY}$, where $M_{\rm SUSY} = 0.1$–$1$ TeV denotes a typical soft SUSY-breaking mass for the $U(1)_Y$ and $SU(2)_L$ gauginos, $\tilde{B}$ and $\tilde{W}_{1,2,3}$, and for the left-handed sneutrinos, $\tilde{\nu}_{e,\mu,\tau}$. As an illustrative scenario, we consider that $m_N$ is much larger than the superpotential $\hat{H}_u\hat{H}_d$-mixing parameter $\mu$ and that $\tilde{\mathbf{M}}^2_{L,E}$ and $\mathbf{A}_e$ are flavor conserving, e.g. proportional to $\mathbf{1}$ at the energy-scale $m_N$.

 

Within the above simplified but realistic framework, we may calculate the leading effects of SLFV in the lowest order of a series expansion of $v_u$ and $m_N^{-1}$. We ignore charged Higgs effects which are subdominant in such an expansion. Detailed analytic results including this and other subleading contributions will be given in a separate communication [18]. The Feynman graphs that contribute to $\gamma l' l$ and $Z l' l$ couplings and box diagrams to leading order in the $\mathrm{SU}(2)_L$ gauge coupling $g_w$ and the neutrino Yukawa coupling $\mathbf{h}_\nu$ are shown in Fig. 1. The pertinent transition amplitudes may be cast into the form

$$\begin{aligned} \mathcal{T}_\mu^{\gamma l' l} &= \frac{e\alpha_w}{8\pi M_W^2}\bar{l}'(F_\gamma^{l'l} q^2 \gamma_\mu P_L + G_\gamma^{l'l} i\sigma_{\mu\nu}q^\nu m_l P_R)l, \\ \mathcal{T}_\mu^{Z l' l} &= \frac{g_w \alpha_w}{8\pi\cos\theta_w} F_Z^{l'l}\bar{l}'\gamma_\mu P_L l, \\ \mathcal{T}_l^{l' l_1 l_2} &= -\frac{\alpha_w^2}{4M_W^2} F_{\rm box}^{l l' l_1 l_2}\bar{l}'\gamma_\mu P_L l \bar{l}_1 \gamma^\mu P_L l_2, \end{aligned} \tag{3}$$

where $P_{L(R)} = \frac{1}{2}[1-(+)\gamma_5]$, $\alpha_w = g_w^2/(4\pi)$, $e$ is the electromagnetic coupling constant, $M_W = g_w\sqrt{v_u^2 + v_d^2}/2$ is the $W$-boson mass, $\theta_w$ is the weak mixing angle and $q = p_{l'} - p_l$ is the photon momentum. In addition, the form factors $F_\gamma^{l'l}$, $G_\gamma^{l'l}$, $F_Z^{l'l}$ and $F_{\rm box}^{ll'l_1l_2}$ receive contributions from both the heavy neutrinos $N_{1,2,3}$ and the right-handed sneutrinos $\tilde{N}_{1,2,3}$. In the Feynman gauge [19], these are individually given by

$$(F_\gamma^{l'l})^N = \frac{\mathbf{\Omega}_{l'l}}{6s_\beta^2}\ln\frac{m_N^2}{M_W^2}, \qquad (F_\gamma^{l'l})^{\tilde{N}} = \frac{\mathbf{\Omega}_{l'l}}{3s_\beta^2}\ln\frac{m_N^2}{\tilde{m}_h^2}, \tag{4}$$

$$\begin{aligned} (G_\gamma^{l'l})^N &= -\mathbf{\Omega}_{l'l}\left(\frac{1}{6s_\beta^2} + \frac{5}{6}\right), \\ (G_\gamma^{l'l})^{\tilde{N}} &= \mathbf{\Omega}_{l'l}\left(\frac{1}{6s_\beta^2} + f\right), \end{aligned} \tag{5}$$

$$\begin{aligned} (F_Z^{l'l})^N &= -\frac{3\mathbf{\Omega}_{l'l}}{2}\ln\frac{m_N^2}{M_W^2} - \frac{(\mathbf{\Omega}^2)_{l'l}}{2s_\beta^2}\frac{m_N^2}{M_W^2}, \\ (F_Z^{l'l})^{\tilde{N}} &= \frac{\mathbf{\Omega}_{l'l}}{2}\ln\frac{m_N^2}{\tilde{m}_1^2} + \frac{(\mathbf{\Omega}^2)_{l'l}}{4s_\beta^2}\frac{m_N^2}{M_W^2}\ln\frac{m_N^2}{\tilde{m}_2^2}, \end{aligned} \tag{6}$$

$$\begin{aligned} (F_{\rm box}^{ll'l_1l_2})^N &= -\mathbf{\Omega}_{l'l}\delta_{l_1l_2} - \mathbf{\Omega}_{l_1l}\delta_{l'l_2} \\ &\quad + \frac{1}{4s_\beta^4}(\mathbf{\Omega}_{l'l}\mathbf{\Omega}_{l_1l_2} + \mathbf{\Omega}_{l_1l}\mathbf{\Omega}_{l'l_2})\frac{m_N^2}{M_W^2}, \\ (F_{\rm box}^{ll'l_1l_2})^{\tilde{N}} &= -\frac{M_W^2}{\tilde{m}^2}(\mathbf{\Omega}_{l'l}\delta_{l_1l_2} + \mathbf{\Omega}_{l_1l}\delta_{l'l_2}) \\ &\quad + \frac{1}{4s_\beta^4}(\mathbf{\Omega}_{l'l}\mathbf{\Omega}_{l_1l_2} + \mathbf{\Omega}_{l_1l}\mathbf{\Omega}_{l'l_2})\frac{m_N^2}{M_W^2}. \end{aligned} \tag{7}$$

In the above, it is $s_\beta \equiv \sin\beta$, $\tilde{m}_W^2 = \max(M_{\tilde{W}}^2, g_w^2 v_u^2/2)$, $\tilde{m}_h^2 = \max(\mu^2, g_w^2 v_u^2/2)$, $\tilde{m}_{1,2}^2 = \max(\tilde{m}_{W,h}^2, M_{\tilde{\nu}}^2)$ and $\tilde{m}^2 = \max(2M_{\tilde{\nu}}^2, \tilde{m}_W^2)$, where $M_{\tilde{\nu}}$ is a common soft SUSY mass for $\tilde{\nu}_{e,\mu,\tau}$. Moreover, the loop function $f$ given in (5) is a lengthy expression involving all the above parameters [18]. In the SUSY limit which requires a vanishing $\mu$ parameter and $\tan\beta = 1$ [20,21], $\tilde{m}_{W,h}^2$, $\tilde{m}_{1,2}^2$ and $\tilde{m}^2$ all tend to $M_W^2 = g_w^2 v_u^2/2$ and $f \to 5/6$.

It is now important to notice that the photonic dipole form factor $G_\gamma^{l'l}$ vanishes in the SUSY limit when the heavy neutrino and sneutrino contributions given in (5), $(G_\gamma^{l'l})^N$ and $(G_\gamma^{l'l})^{\tilde{N}}$, are added together. This result is a direct consequence of a nonrenormalization theorem of SUSY [22]. Thus, if SUSY is the dominant source for LFV in nature, photonic charged-lepton decays, such as $\mu \to e\gamma$, $\tau \to e\gamma$ and $\tau \to \mu\gamma$, become practically forbidden transitions. In reality, SUSY is softly broken and these decay rates will strongly depend on the details of the soft SUSY-breaking sector. It is remarkable here, however, that even a flavor conserving soft SUSY-breaking sector for the low-scale seesaw models under study can cause sizeable LFV.

Another important observation pertains to the actual strength of the neutrino Yukawa couplings $\mathbf{h}_\nu$. If $|\mathbf{h}_\nu| \gtrsim g_w \approx 0.65$, then terms of order $(\mathbf{\Omega}_{l'l})^2 \propto (\mathbf{h}_\nu^\dagger \mathbf{h}_\nu)_{l'l}^2$ will dominate the $Z$-boson and box-mediated transition amplitudes given in (3) [14]. Therefore, the central goal of this study is to identify the key phenomenological features that would enable one to distinguish whether SLFV originates from small or potentially large neutrino Yukawa couplings.

To obtain predictions for the LFV observables $B(\mu^- \to e^-\gamma)$, $B(\tau^- \to e^-\gamma)$, $B(\mu^- \to e^-e^-e^+)$, $B(\tau^- \to e^-e^-e^+)$ and $B(\tau^- \to e^-\mu^-\mu^+)$, we use the analytic expressions (4.9) and (4.10) of [14], along with the form factors given in (4)–(7). The predicted rate $R_{\mu e}$ for coherent $\mu \to e$ conversion in a nucleus with atomic numbers $(N, Z)$ may be calculated by

$$R_{\mu e} = \frac{\alpha^3\alpha_w^4 m_\mu^5 |F(-m_\mu^2)|^2}{16\pi^2 M_W^4 \Gamma_{\rm capt}}\frac{Z_{\rm eff}^4}{Z}|Q_W|^2, \tag{8}$$

where $\alpha = e^2/(4\pi)$, $Z_{\rm eff}$ is the effective atomic number of coherence [23], $F(-m_\mu^2)$ is a nucleus-dependent nuclear form factor [24] and $\Gamma_{\rm capt}$ is the total muon capture rate. In addition, $Q_W = V_u(2Z+N) + V_d(Z+2N)$ is the weak matrix element, where

$$\begin{aligned} V_u &= -\tfrac{2}{3}s_w^2(F_\gamma^{\mu e} + G_\gamma^{\mu e} + F_Z^{\mu e}) + \tfrac{1}{4}(F_Z^{\mu e} - F_{\rm box}^{\mu euu}), \\ V_d &= \tfrac{1}{3}s_w^2(F_\gamma^{\mu e} + G_\gamma^{\mu e} + F_Z^{\mu e}) - \tfrac{1}{4}(F_Z^{\mu e} + F_{\rm box}^{\mu edd}), \end{aligned} \tag{9}$$

with $s_w \equiv \sin\theta_w$. The leading contributions to the form factors $F_{\rm box}^{\mu euu}$ and $F_{\rm box}^{\mu edd}$ pertinent to the up and down quarks, respectively, are obtained by calculating the $W$- and $\tilde{W}$-mediated box graphs analogous to Fig. 1. More explicitly, we find

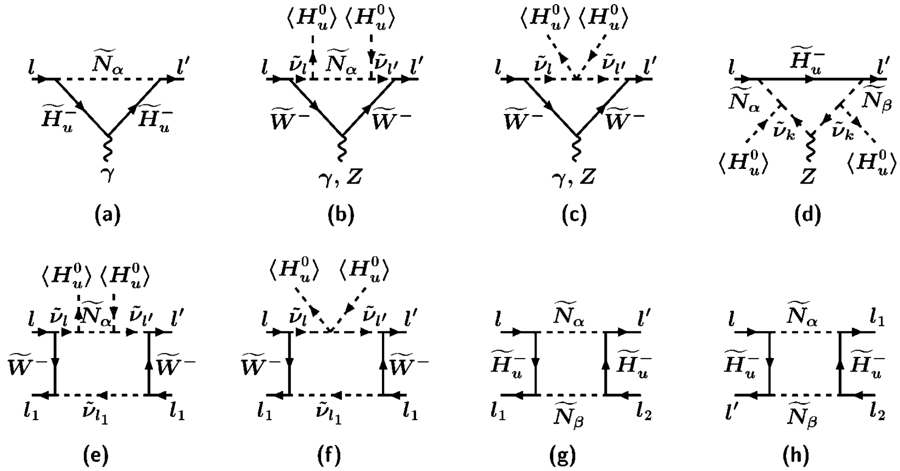


FIG. 1. Feynman graphs giving rise to leading SLFV effects in the lowest order of an expansion in $\langle H_u^0\rangle$ and $m_N^{-1}$. Not shown are diagrams obtained by replacing the tilted SUSY states $\tilde{H}_u^-$, $\tilde{W}^-$, $\tilde{N}_\alpha$ and $\tilde{\nu}_l$ with their untilted counterparts.

$$\begin{aligned}(F_{\rm box}^{\mu euu})^N &= -4(F_{\rm box}^{\mu edd})^N = 4\mathbf{\Omega}_{e\mu},\\ (F_{\rm box}^{\mu euu})^{\tilde{N}} &= \frac{2M_W^2\tilde{m}_W^2}{\tilde{M}_Q^4}\mathbf{\Omega}_{e\mu},\\ (F_{\rm box}^{\mu edd})^{\tilde{N}} &= -\frac{M_W^2}{2\tilde{M}_Q^2}\mathbf{\Omega}_{e\mu},\end{aligned} \tag{10}$$

where we assumed that $|\tilde{m}_W| \ll \tilde{M}_Q \approx M_{\tilde{\nu}}$, with $\tilde{M}_Q$ being a common soft SUSY-breaking mass for the left-handed up and down squarks in the loop.

In our numerical estimates, we fix $\tilde{M}_Q = M_{\tilde{\nu}} = -\mu = 200$ GeV, $M_{\tilde{W}} = 100$ GeV and $\tan\beta = 3$ [25]. We first analyze the impact of SLFV on $\mu \to e$ transitions. We consider a conservative scenario with $\mathbf{\Omega}_{ee} = \mathbf{\Omega}_{\mu\mu} = \mathbf{\Omega}_{e\mu}$ and $\mathbf{\Omega}_{\tau\tau} = 0$, which yields the weakest limits on $\mathbf{\Omega}_{e\mu}$. To this end, we present in Fig. 2 exclusion contours for $\mathbf{\Omega}_{e\mu}$ versus $m_N$ derived from present experimental limits and future sensitivities: $B(\mu^- \to e^-\gamma) < 1.2 \times 10^{-11}$ [26] (upper horizontal line), $B(\mu^- \to e^-\gamma) \sim 10^{-13}$ [6] (lower horizontal line), $B(\mu^- \to e^-e^-e^+) < 10^{-12}$ [26] (dashed line). We also include constraints from the nonobservation of $\mu \to e$ conversion in ${}^{48}_{22}$Ti and ${}^{197}_{79}$Au [27], $R_{\mu e}^{\rm Ti} < 4.3 \times 10^{-12}$ [28] (dash-dotted lines) and $R_{\mu e}^{\rm Au} < 7 \times 10^{-13}$ [29] (dash-double-dotted line), as well as potential limits from a future sensitivity to $R_{\mu e}^{\rm Ti}$ at the $10^{-18}$ level [7] (lower dash-dotted line). The areas lying above or within the contours are excluded by the above considerations. In the upper panel of Fig. 2, the loop effects from both $N_{1,2,3}$ and $\tilde{N}_{1,2,3}$ are considered, whereas in the lower one only those from $N_{1,2,3}$ are taken into account. Finally, the diagonal dotted line indicates the regime where terms $\propto (\mathbf{\Omega}_{l'l})^2$ dominate the LFV observables, while the area above the diagonal solid line represents a nonperturbative regime with $\mathrm{Tr}(\mathbf{h}_\nu^\dagger\mathbf{h}_\nu) > 4\pi$, which limits the validity of our predictions.

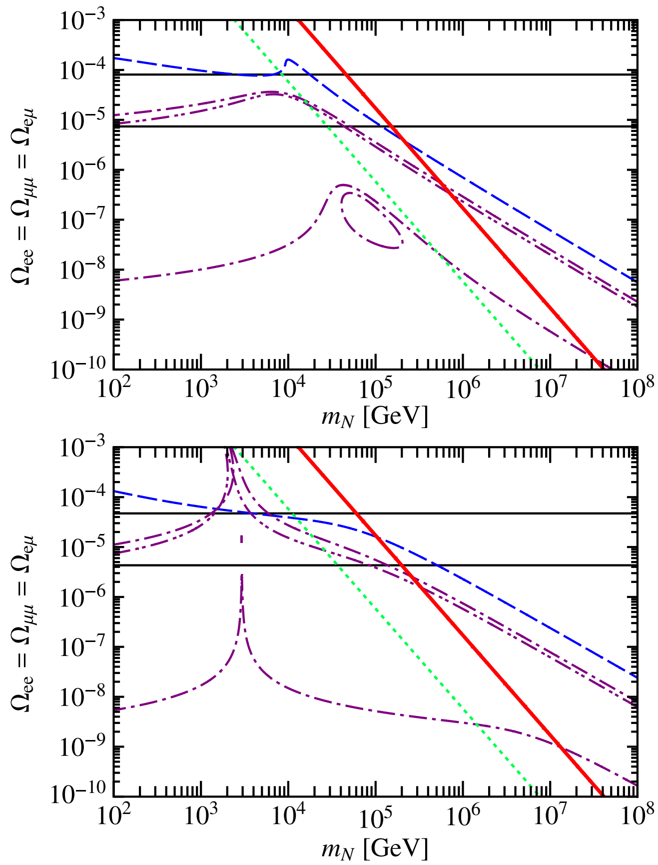


FIG. 2 (color online). Exclusion contours of $\mathbf{\Omega}_{e\mu}$ versus $m_N$ derived from experimental limits on $B(\mu^- \to e^-\gamma)$ (horizontal solid lines), $B(\mu^- \to e^-e^-e^+)$ (dashed line) and $\mu \to e$ conversion in titanium (dash-dotted lines) and Gold (dash-double-dotted line), assuming $\mathbf{\Omega}_{ee} = \mathbf{\Omega}_{\mu\mu} = \mathbf{\Omega}_{e\mu}$ and $\mathbf{\Omega}_{\tau\tau} = 0$. In the lower panel, the quantum effects due to $\tilde{N}_{1,2,3}$ have been ignored. The diagonal solid and dotted lines are defined by the conditions $\mathrm{Tr}(\mathbf{h}_\nu^\dagger\mathbf{h}_\nu) = 4\pi$ and $\mathrm{Tr}(\mathbf{h}_\nu^\dagger\mathbf{h}_\nu) = g_w^2$, respectively. The areas that lie above or within the contours are excluded; see the text for more details.

Figure 2 also shows the importance of synergy among the different LFV experiments. In particular, we find an area of cancellation in the predicted value for $R_{\mu e}$ for $m_N \sim 3$ TeV in the non-SUSY case (lower panel). This area is covered to a good extent by the present limits from the $\mu \to eee$ experiment and by the current and future [6] exclusion limits on $B(\mu \to e\gamma)$. Most interestingly, the projected PRISM experiment for $R_{\mu e}^{\rm Ti} \sim 10^{-18}$ [7] will reach sensitivities to the unprecedented level of $\mathbf{\Omega}_{e\mu} \sim 10^{-10}$ and $m_N \sim 10^8$ GeV. In the kinematic regime of large Yukawa couplings, we see that the experiments for $\mu \to e$ conversion in nuclei offer the highest sensitivity. In the same regime, we observe that the derived bounds on $\mathbf{\Omega}_{e\mu}$ and $m_N$ are much stricter in the SUSY rather than in the non-SUSY case (lower panel). The reason is that in this large $m_N$ domain, $(F_Z^{l'l})^{\tilde N}$ prevails over $(F_Z^{l'l})^N$ and adds constructively to the dominant contribution $(F_{\rm box}^{\mu euu})^N$.

We now turn our attention to $\tau$ LFV, analyzing a conservative scenario with $\mathbf{\Omega}_{ee} = \mathbf{\Omega}_{\tau\tau} = \mathbf{\Omega}_{e\tau}$ and $\mathbf{\Omega}_{\mu\mu} = 0$ [30]. In Fig. 3 we display exclusion contours of $\mathbf{\Omega}_{e\tau}$ versus $m_N$, using the present experimental upper limits [26] on $B(\tau^- \to e^-\gamma) < 1.1 \times 10^{-7}$ (horizontal solid lines), $B(\tau^- \to e^-e^-e^+) < 3.6 \times 10^{-8}$ (dashed lines) and $B(\tau^- \to e^-\mu^-\mu^+) < 3.7 \times 10^{-8}$ (dash-dotted lines). The thick lines show exclusion contours of SLFV, whereas the thin lines of the same pattern are the corresponding contours in the non-SUSY case. As in Fig. 2, the diagonal dotted line indicates the regime where large Yukawa coupling effects dominate, whereas the diagonal solid line places the boundary for nonperturbative dynamics. We see that the current bound on $B(\tau \to e\gamma)$ is less sensitive to SLFV, due to the screening coming from the right-handed sneutrinos in the loop. Moreover, given the constraints [16], a positive signal for $B(\tau^- \to e^-e^-e^+)$ close to the present upper bound will signify that SLFV originates from rather large Yukawa couplings and $m_N \gtrsim 3$ TeV.

In summary, we have shown that low-mass right-handed sneutrinos can sizably contribute to observables of LFV.

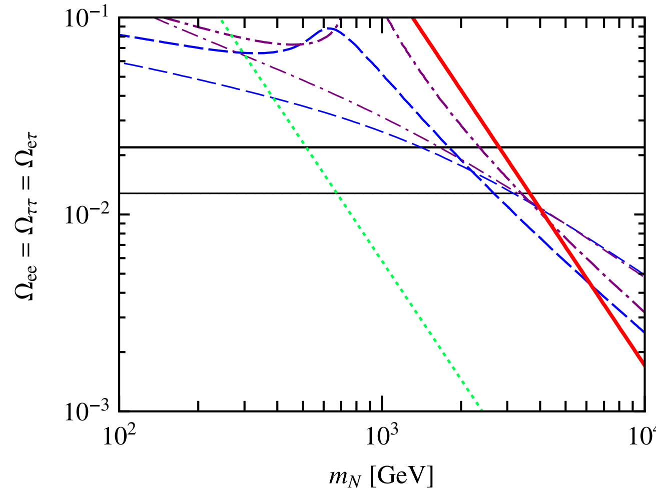


FIG. 3 (color online). Exclusion contours of $\mathbf{\Omega}_{e\tau}$ versus $m_N$ derived from present experimental upper limits on $B(\tau^- \to e^-\gamma)$ (horizontal solid lines), $B(\tau^- \to e^-e^-e^+)$ (dashed lines) and $B(\tau^- \to e^-\mu^-\mu^+)$ (dash-dotted lines), assuming that $\mathbf{\Omega}_{ee} = \mathbf{\Omega}_{\tau\tau} = \mathbf{\Omega}_{e\tau}$ and $\mathbf{\Omega}_{\mu\mu} = 0$. The diagonal solid and dotted lines are defined by the conditions $\mathrm{Tr}(\mathbf{h}_\nu^\dagger \mathbf{h}_\nu) = 4\pi$ and $\mathrm{Tr}(\mathbf{h}_\nu^\dagger \mathbf{h}_\nu) = g_w^2$, respectively. More details are given in the text.

Thanks to SUSY, they can significantly screen the respective effect of the heavy neutrinos on the photonic $\mu$ and $\tau$ decays. Hence SLFV can be probed more effectively in present and future experiments of $\mu \to e$ conversion in nuclei. The 3-body decay observables, such as $\mu \to eee$ and $\tau \to eee$, provide valuable complementary information on LFV. In particular, the former eliminates a kinematic region that remains unprobed in the non-SUSY case by $\mu \to e$ conversion experiments. Therefore, plans for potentially upgrading the $\mu \to eee$ experiment should be followed with the same degree of vigor in the community. In the same vein, the implications of SLFV in semileptonic $\tau$ decays and in processes involving $K$ and $B$ mesons should also be explored. We plan to report progress on these issues in the near future.


[1] For reviews, see H. P. Nilles, Phys. Rep. **110**, 1 (1984); H. Haber and G. Kane, Phys. Rep. **117**, 75 (1985).

[2] P. Minkowski, Phys. Lett. **B67**, 421 (1977); M. Gell-Mann, P. Ramond, and R. Slansky, in *Supergravity*, edited by D. Z. Freedman and P. van Nieuwenhuizen (North-Holland, Amsterdam, 1979); T. Yanagida, in *Proc. of the Workshop on the Unified Theory and the Baryon Number in the Universe*, edited by O. Sawada and A. Sugamoto (Tsukuba, Japan, 1979); R. N. Mohapatra and G. Senjanović, Phys. Rev. Lett. **44**, 912 (1980).

[3] F. Borzumati and A. Masiero, Phys. Rev. Lett. **57**, 961 (1986).

[4] J. Hisano, T. Moroi, K. Tobe, and M. Yamaguchi, Phys. Rev. D **53**, 2442 (1996).

[5] T. P. Cheng and L. F. Li, Phys. Rev. Lett. **45**, 1908 (1980).

[6] S. Ritt (MEG Collaboration), Nucl. Phys. B, Proc. Suppl. **162**, 279 (2006).

[7] Y. Kuno, Nucl. Phys. B, Proc. Suppl. **149**, 376 (2005).

[8] D. Wyler and L. Wolfenstein, Nucl. Phys. **B218**, 205 (1983).

[9] R. N. Mohapatra and J. W. F. Valle, Phys. Rev. D **34**, 1642 (1986); S. Nandi and U. Sarkar, Phys. Rev. Lett. **56**, 564 (1986).

[10] G. C. Branco, W. Grimus, and L. Lavoura, Nucl. Phys.

**B312**, 492 (1989).

[11] A. Pilaftsis, Z. Phys. C **55**, 275 (1992).

[12] A. Pilaftsis, Phys. Rev. Lett. **95**, 081602 (2005).

[13] J. Bernabéu, A. Santamaria, J. Vidal, A. Mendez, and J. W. F. Valle, Phys. Lett. B **187**, 303 (1987); J. G. Körner, A. Pilaftsis, and K. Schilcher, Phys. Lett. B **300**, 381 (1993).

[14] A. Ilakovac and A. Pilaftsis, Nucl. Phys. **B437**, 491 (1995).

[15] F. Deppisch and J. W. F. Valle, Phys. Rev. D **72**, 036001 (2005).

[16] For the diagonal entries, we conservatively assume that $\Omega_{ee,\mu\mu,\tau\tau} \lesssim 10^{-2}$ [17].

[17] S. Bergmann and A. Kagan, Nucl. Phys. **B538**, 368 (1999); F. del Aguila, J. de Blas, and M. Perez-Victoria, Phys. Rev. D **78**, 013010 (2008).

[18] A. Ilakovac and A. Pilaftsis (unpublished).

[19] We note that unlike the off-shell form factors, physical amplitudes do not depend on the choice of the gauge.

[20] See Appendix B.2 of Haber and Kane in [1].

[21] We do not consider here the infrared singular SUSY limit, without electroweak-symmetry breaking for $\mu \neq 0$.

[22] S. Ferrara and E. Remiddi, Phys. Lett. **B53**, 347 (1974).

[23] H. C. Chiang, E. Oset, T. S. Kosmas, A. Faessler, and J. D. Vergados, Nucl. Phys. **A559**, 526 (1993).

[24] R. Kitano, M. Koike, and Y. Okada, Phys. Rev. D **66**, 096002 (2002).

[25] For this choice of parameter values, the residual loop function $f$ is given by $f \approx M_W^2/(3\tilde{m}_2^2)$.

[26] C. Amsler *et al.*, Phys. Lett. B **667**, 1 (2008).

[27] To get predictions for $R_{\mu e}$, we use the values for $Z_{\rm eff}$, $|F(-m_\mu^2)|$ and $\Gamma_{\rm capt}$ given in [24].

[28] C. Dohmen *et al.* (SINDRUM II Collaboration), Phys. Lett. B **317**, 631 (1993).

[29] W. Bertl *et al.*, Eur. Phys. J. C **47**, 337 (2006).

[30] The limits derived for the complementary scenario with $\mathbf{\Omega}_{\mu\mu} = \mathbf{\Omega}_{\tau\tau} = \mathbf{\Omega}_{\mu\tau}$ and $\mathbf{\Omega}_{ee} = 0$ are quite similar.